Charge Changes in Loop 2 Affect the Thermal Unfolding of the Myosin Motor Domain Bound to F-Actin†

Michael A. Ponomarev,‡ Marcus Furch,§ Dmitrii I. Levitsky,‡,|| and Dietmar J. Manstein*,§

A.N.Bach Institute of Biochemistry, Russian Academy of Sciences, Leninsky prosp. 33, Moscow 117071, Russia, Max-Planck-Institut für Medizinische Forschung, Jahnstrasse 29, 69120 Heidelberg, Germany, and A.N.Belozersky Institute of Physico-Chemical Biology, Moscow State University, Moscow 119899, Russia

Received October 18, 1999; Revised Manuscript Received January 20, 2000

ABSTRACT: The thermal unfolding of *Dictyostelium discoideum* myosin head fragments with alterations in the actin-binding surface loop 2 was studied by differential scanning calorimetry. Lengthening of loop 2 without concomitant charge changes led to decreases in the transition temperature of not more than 1.8 °C. Insertions with multiple positive or negative charges had a stronger destabilizing effect and led to reductions in the thermal transition temperature of up to 3.7 °C. In the presence of nucleotide, most mutants displayed similar or higher transition temperatures than M765. Only constructs M765(11/+6) and M765(20/+12) with long positively charged inserts showed transition temperatures that were more than 2 °C below the values measured for M765 in the presence of ADP, ADP−V_i, and ADP−BeF_3. Interaction with F-actin in the presence of ADP shifted the thermal transition of M765 by 6 °C, from 49.1 to 55.1 °C. The actin-induced increase in thermal stability varied between 1.2 and 9.1 °C and showed a strong correlation with the mutant constructs' affinity for actin. Our results show that length and charge changes in loop 2 do not significantly affect nucleotide-induced structural changes in the myosin motor domain, but they affect structural changes that occur when the motor domain is strongly bound to actin and affect the coupling between the actin- and nucleotide-binding sites.

Myosins are complex multidomain proteins that interact with actin filaments and adenosine triphosphate (ATP)[1] to produce mechanical force and movement. The N-terminal globular head domain contains the binding sites for the myosin light chains and has the catalytic and actin-binding properties required for myosin motor activity (*1, 2*). Myosin II has been characterized in many systems, and although myosin isoforms are highly homologous throughout most of the catalytic domain, their enzymatic properties are variable as determined by their ATPase rates and unloaded shortening velocities (*3*). It has been proposed that two solvent-exposed, proteolytically sensitive surface loops that lie near the ATP (loop 1) and actin (loop 2) binding sites could be critical for modulating myosin's kinetic activities (*4*).

Structural and biochemical studies have shown that loop 2, a lysine-rich surface segment of the myosin motor domain, interacts directly with the negatively charged amino-terminal part of actin, and this electrostatic interaction is mainly responsible for the "weak" binding of the myosin head to F-actin (*5*−*10*). Molecular genetic modifications of loop 2 have been shown to alter myosin's affinity for actin and its actin-activated ATPase activity. Experiments with chimeric *Dictyostelium discoideum* myosins, in which loop 2 was substituted by that from myosins from other species, showed a good correlation between the actin-activated ATPase activities of these chimeras and the activities of the myosins from which the loop sequences were derived (*11*). More recently, nine mutant constructs of myosin head fragment M765 were produced by site-directed mutagenesis and characterized kinetically (*12*). M765 is a soluble myosin head fragment truncated after residue 765, which represents the isolated motor domain of *Dictyostelium* myosin II. In comparison to native *Dictyostelium* myosin, the loop 2 region of the mutant constructs was modified to carry up to 20 additional amino acids and charge variations from −1 to +12. It was shown that alterations in loop 2 do not affect binding of nucleotide, but they do affect the actin-binding properties of M765. For example, mutant constructs with 4−12 extra positive charges displayed a significant increase in actin-activated ATPase activity and in affinity for actin, in comparison with the wild-type construct M765. It was proposed from these kinetic data that the introduction of extra lysine residues in loop 2 not only increases the rate of formation of the initial collision complex with actin which is governed by long-range ionic interactions, but also affects the transition from a "weak" actin-binding state (A-state) to a "strong" binding state (R-state). This A-to-R transition involves major structural rearrangements with formation of

† Supported by the Max-Planck-Society, INTAS-RFBR Grant IR-97-577, and Grant MA 1081/5-1 to D.J.M. from the Deutsche Forschungsgemeinschaft.

* To whom correspondence should be addressed. Phone: (+49-6221) 486 212. Fax: (+49-6221) 486 437. E-mail: manstein@mpimf-heidelberg.mpg.de.

‡ Russian Academy of Sciences.

§ Max-Planck-Institut für Medizinische Forschung.

|| Moscow State University.

[1] Abbreviations: acto-S1, complex of actin and S1; ATP, adenosine-5′-triphosphate; BeF_3, beryllium fluoride; DSC, differential scanning calorimetry; EDTA, ethylenediamine tetraacetic acid; M765, *D. discoideum* myosin II motor domain; S1, subfragment 1 of myosin; V_i, orthovanadate.

10.1021/bi992420a CCC: $19.00
Published on Web 03/24/2000

additional actomyosin contacts and internal conformational changes involving both hydrophobic and ionic interactions (*12*). It is generally assumed that charge changes in loop 2 affect the conformation of myosin heads that are "strongly" bound to F-actin. To check this assumption, we used differential scanning calorimetry (DSC) to analyze the thermal unfolding of M765 mutants with alterations in loop 2.

DSC is the most effective and commonly employed method to study the thermal unfolding of proteins (*13, 14*). This method was successfully used for probing the conformational changes that occur in the myosin head due to formation of stable ternary complexes with ADP and P_i analogues, such as orthovanadate (V_i), beryllium fluoride (BeF_3), or aluminum fluoride (AlF_4). These complexes are stable analogues of the intermediate states of myosin-catalyzed Mg^{2+}−ATPase reaction (*15*−*17*), and therefore, they are often used for probing the conformational changes occurring in the myosin head in the course of the ATPase reaction. It has been shown by DSC that the formation of a complex with ADP−V_i or ADP−BeF_3 causes a global change in the conformation of S1 that is reflected in an increased thermal stability of the protein (*18*−*20*). It has also been concluded from DSC experiments with recombinant *D. discoideum* myosin head fragments that structural changes revealed by DSC, which are due to ADP binding and to the formation of stable ternary complexes with ADP and P_i analogues, occur mainly in the globular motor portion of the head (*21*). Moreover, DSC was also used for probing the structural changes that occur in the myosin head due to its strong binding to F-actin in the presence of ADP. It was shown that the binding of skeletal S1 to F-actin significantly increased the thermal stability of S1 (*22*).

In the present study we applied these DSC approaches to examine mutant constructs of *D. discoideum* myosin head fragment M765 with alterations in loop 2. The names of the mutant constructs reflect changes in the length and charge of loop 2. For example, M765(11/0) indicates the insertion of 11 amino acids with no additional charge, and M765-(8/+4) indicates the insertion of 8 amino acids including 4 positively charged lysine residues. The kinetic properties of all constructs used in this study, with the exception of M765-(20/−10), have been reported previously (*12*). The thermal unfolding of mutant myosin head fragments was measured in the absence of nucleotides, in the presence of ADP, and in the ternary complexes with ADP and P_i analogues (V_i, BeF_3). The thermal stability of these fragments complexed with F-actin in the presence of ADP was also studied. The main calorimetric parameters extracted from these data were the transition temperature, T_m, the calorimetric enthalpy, ΔH_{cal}, and the width at the half-height of the transition, $\Delta T_{0.5}$, which is a relative measure for the cooperativity of the transition.

MATERIAL AND METHODS

Expression and Purification of Mutant Myosin Head Fragments. Plasmids for the production of recombinant myosin motor domains were derived from the extrachromosomal vector pDXA-3H (*23*). Expression vectors for the production of myosin head fragments with loop 2 insertions were created as described previously (*12*). *Dictyostelium* transformants were grown at 21 °C in HL-5C (*12*). Transformants were selected and screened for the production of the recombinant myosin motor domains, and the His-tagged motor domains were purified as described by Manstein and Hunt (*24*). Yields of up to 5 mg of homogeneous protein/g of cells were obtained.

Preparation of the Complexes of Myosin Head Fragments with ADP and P_i Analogues. Trapping of ADP by different phosphate analogues (V_i, BeF_3) was performed by the methods described for the preparation of stable ternary complexes S1·ADP·V_i and S1·ADP·BeF_3 (*15, 17, 20*). To obtain these complexes, myosin head fragments (1 mg/mL) were incubated with 1 mM ADP and 0.4 mM V_i or BeF_3 for 30 min at 20 °C in a medium containing 30 mM Hepes, pH 7.3, and 1 mM $MgCl_2$. Beryllium fluoride complexes were obtained by addition of 0.4 mM $BeCl_2$ in the presence of 5 mM NaF. The Ca^{2+}/high salt−ATPase activity was followed to confirm the formation of the complexes. The ATPase activity of myosin head fragments complexed with ADP−V_i or ADP−BeF_3 did not exceed 3−5% of the activity of the unmodified proteins.

Preparation of the Complexes of Myosin Head Fragments with F-Actin. Actin was prepared from rabbit skeletal muscle acetone powder (*25*). Monomeric G-actin was stored in low-strength buffer composed of 2 mM Tris−HCl, pH 8.0, 0.2 mM ATP, 0.2 mM $CaCl_2$, 0.5 mM β-mercaptoethanol, and 0.01% NaN_3 (G-buffer). The concentration of actin was determined spectrophotometrically, using $A^{1\%}$ at 290 nm equal to 6.3. G-actin was polymerized to F-actin in G-buffer by the addition of 4 mM $MgCl_2$. F-actin was stabilized by the addition of a 2-fold molar excess of phalloidin (Sigma) to obtain a better separation of the thermal transitions of actin-bound myosin head fragments and F-actin. Specific binding of this cyclic heptapeptide to F-actin was shown to increase the temperature of the thermal denaturation of F-actin by 14 °C (*26*). A similar effect of phalloidin was observed in our experiments. The complexes of myosin head fragments with F-actin were formed by mixing equal volumes of an F-actin solution and a myosin solution. F-actin solutions contained G-buffer, 2 mM $MgCl_2$, and 1 mM ADP. Myosin solutions contained 30 mM Hepes, pH 7.3, 2 mM $MgCl_2$, and 1 mM ADP. The final concentrations of F-actin and myosin head fragments were 34 and 17 μM, respectively.

Differential Scanning Calorimetry. DSC experiments were performed on a DASM-4M differential scanning microcalorimeter (Institute for Biological Instrumentation, Pushchino, Russia) with cell volumes of 0.48 mL, at a scanning rate of 1 K/min. Prior to DSC experiments the myosin head fragments were dialyzed against 30 mM Hepes, pH 7.3, containing 2 mM $MgCl_2$. Samples were degassed with stirring in an evacuated chamber for 10 min at room temperature before each measurement and immediately loaded into the calorimeter cell. Degassed dialysis buffer was loaded into the reference cell. A mixture of equal volumes of dialysis buffer and G-buffer, both containing 2 mM $MgCl_2$ and 1 mM ADP, was loaded into the reference cell for experiments with the actomyosin complexes. A pressure of 203 kPa (2 atm) of dry nitrogen was always kept over the liquids in the cells throughout the scans to prevent any degassing during heating. The reversibility of the thermal transitions was verified by checking the reproducibility of the calorimetric trace in a second heating of the sample

immediately after cooling from the first scan. The thermal denaturation of all protein samples studied was fully irreversible. The calorimetric traces were corrected for the calorimetric baseline (a background scan collected with buffer in both cells was subtracted from each scan). The temperature dependence of the molar heat capacity was further analyzed and plotted using Origin 5.0 software (MicroCal Inc., Northampton, MA).

Transition temperatures (T_m) were determined from the maximum of the temperature dependence of the molar heat capacity. Calorimetric enthalpies (ΔH_{cal}) were calculated from the area under the excess heat capacity curves. The width at the half-height of the excess heat capacity traces ($\Delta T_{0.5}$) was used for evaluation of the relative cooperativity of the thermal transitions. These parameters are directly available from the experimental calorimetric traces, or after simple treatments such as concentration normalization, chemical baseline correction, and subtraction of instrumental background. Molecular masses from 89.5 kDa for M765 to 91.3 kDa for M765(20/−10) were used for calculation of the excess molar heat capacity of the myosin head fragments.

Stopped-Flow Experiments. Stopped-flow experiments were performed with a Hi-tech SF-61MX stopped-flow spectrophotometer (Salisbury, U.K.) using a 75 W Xe/Hg lamp and a monochromator for wavelength selection. Pyrene fluorescence was excited at 365 nm and emission monitored after passing through a KV 389 nm cutoff filter (Schott, Mainz, Germany). Data were stored and analyzed using software provided by Hi-tech. The experimental buffer was 20 mM MOPS, 5 mM $MgCl_2$, and 100 mM KCl, pH 7.0, and the reaction temperature 20 °C.

RESULTS

Calorimetric Characterization of Mutant Myosin Head Fragments. In the absence of nucleotides most mutant constructs displayed decreased thermostability. The extent of the observed decrease in T_m and ΔH_{cal} correlated well with the number of inserted amino acid residues (Table 1). The introduction of both positive and negative charge appeared to have an additional destabilizing effect. Accordingly, mutant constructs M765(4/−1) and M765(4/+1) with small inserts and charge changes displayed calorimetric parameters similar to those observed for the wild-type construct M765 (T_m = 45.6 °C), whereas the transition temperature for M765(20/−10), M765(11/0), and M765(11/+6) was shifted to lower temperature by 3.0, 1.6, and 3.7 °C, respectively.

Nucleotide-Induced Changes in the Thermal Unfolding of Mutant Myosin Head Fragments. Previous DSC studies performed with skeletal muscle S1 and with *D. discoideum* myosin head fragment M761 have shown that DSC is useful for probing global conformational changes in the myosin motor caused by ligand binding. Formation of stable ternary complexes of the myosin head with ADP and P_i analogues such as V_i, BeF_3, and AlF_4 were shown to cause a significant increase of the thermal stability of the protein, as judged by the values measured for T_m, ΔH_{cal}, and $\Delta T_{0.5}$ (*18, 20, 21*). Figure 1 shows the effects of the formation of the ternary complexes of M765(4/−1) with ADP−V_i and ADP−BeF_3, in comparison with the effect of ADP alone and the nucleotide-free protein. ADP binding increased T_m in the case of M765(4/−1) by 5.6 °C. Nucleotide binding also increased the cooperativity of the transition as indicated by a decrease of $\Delta T_{0.5}$ from 6.1 to 5.4 °C. Formation of the ternary complexes was accompanied by further increases in T_m and cooperativity ($\Delta T_{0.5}$ = 3.3−3.6 °C) (Figure 1). Similar results were obtained with myosin head fragments M765 (Table 1) and M761 (*21*).

The DSC experiments showed that all myosin head fragments with alterations in loop 2 are able to undergo global structural changes due to ADP binding and the formation of stable ternary complexes with ADP and P_i analogues. The addition of nucleotide had a strong stabilizing effect on all mutant constructs, leading to increases in T_m by 3.7−6.5 °C (Table 1). All constructs showed stronger ADP-induced stabilization than the wild-type construct M765 (ΔT_m by 3.5 °C). The nucleotide-induced changes of the calorimetric parameters displayed construct-dependent and in particular charge-related differences (Table 1). The largest shift of 6.5 °C was observed for M765(20/−10) (Figure 2 A). The addition of ADP to constructs M765(8/0), M765-

Table 1: Calorimetric Parameters Obtained from the DSC Data for Mutant Myosin Head Fragments Alone or in Their Complexes with Nucleotides[a]

myosin head fragment or complex	T_m (°C)	ΔH_{cal} (kcal/mol)	$\Delta T_{0.5}$ (°C)
M765	45.6	210	5.7
M765·ADP	49.1	220	5.2
M765·ADP·BeF_3	52.7	240	3.7
M765·ADP·V_i	55.4	250	3.8
M765(20/−10)	42.6	180	4.9
M765(20/−10)·ADP	49.1	185	4.4
M765(20/−10)·ADP·BeF_3	51.0	230	3.9
M765(20/−10)·ADP·V_i	50.8	200	4.1
M765(4/−1)	45.5	210	6.1
M765(4/−1)·ADP	51.1	225	5.4
M765(4/−1)·ADP·BeF_3	52.5	215	3.3
M765(4/−1)·ADP·V_i	53.2	230	3.6
M765(8/0)	43.8	210	5.0
M765(8/0)·ADP	49.4	215	5.1
M765(8/0)·ADP·BeF_3	50.7	240	4.9
M765(8/0)·ADP·V_i	na	na	na
M765(11/0)	44.0	200	4.8
M765(11/0)·ADP	49.3	205	4.5
M765(11/0)·ADP·BeF_3	52.0	215	4.5
M765(11/0)·ADP·V_i	52.8	230	3.8
M765(4/+1)	45.1	190	5.6
M765(4/+1)·ADP	48.8	190	5.3
M765(4/+1)·ADP·BeF_3	52.1	220	3.7
M765(4/+1)·ADP·V_i	52.6	210	3.8
M765(8/+4)	44.0	190	5.2
M765(8/+4)·ADP	48.0	185	6.4
M765(8/+4)·ADP·BeF_3	50.9	200	4.4
M765(8/+4)·ADP·V_i	51.4	220	3.8
M765(11/+6)	41.9	180	4.2
M765(11/+6)·ADP	45.8	160	4.1
M765(11/+6)·ADP·BeF_3	na	na	na
M765(11/+6)·ADP·V_i	51.7	215	3.7
M765(20/+12)	42.8	175	7.2
M765(20/+12)·ADP	47.0	180	6.1
M765(20/+12)·ADP·BeF_3	48.3	185	6.9
M765(20/+12)·ADP·V_i	51.5	190	3.9

[a] Values obtained from two to four independent measurements are shown. The absolute error of the given T_m values did not exceed ±0.2 °C. The relative error of the given ΔH_{cal} values did not exceed ±8%. The parameter $\Delta T_{0.5}$, the width at the half-height of the thermal transition, is a relative measure for the cooperativity of the transition. "na" means data were not analyzed. Experimental conditions for all measurements: 30 mM Hepes, 1 mM $MgCl_2$, pH 7.3.

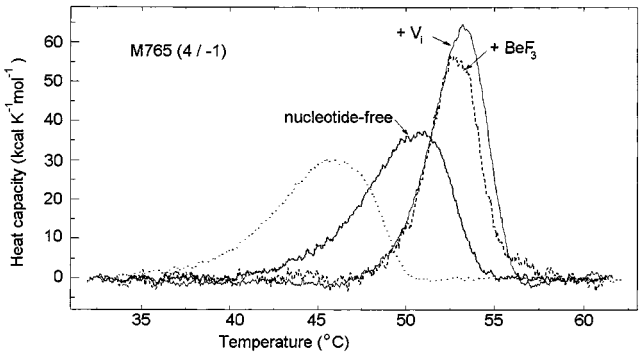

FIGURE 1: DSC scans of M765(4/−1) in the absence of nucleotides (dotted line), in the presence of 1 mM ADP (ADP, solid line), in the presence of 1 mM ADP, 5 mM NaF, and 0.4 mM $BeCl_2$ (BeF_3, dashed line), and in the presence of 1 mM ADP and 0.4 mM V_i (V_i, solid line). The protein concentration was 1 mg/mL. Other conditions: 30 mM Hepes, pH 7.3, and 1 mM $MgCl_2$. The heating rate was 1 K/min. The parameters derived from the data are shown in Table 1.

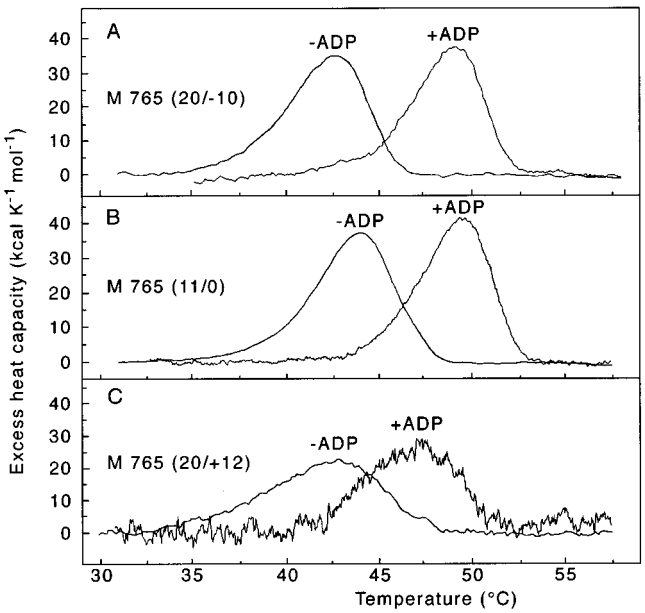

FIGURE 2: DSC scans of M765(20/−10) (A), M765(11/0) (B), and M765(20/+12) (C) in the presence of 1 mM ADP. Curves shown by dotted lines were obtained in the absence of ADP. Conditions were the same as in Figure 1. The parameters derived from the data are shown in Table 1.

(11/0), and M765(4/−1) led to a shift of 5.3−5.6 °C (Figure 2B). The smallest ADP-induced shift of the thermal transition to higher temperature (ΔT_m) was observed for mutant constructs with additional positive charges in loop 2. The values of ΔT_m for M765(4/+1), M765(8/+4), M765(11/+6), and M765(20/+12) varied between 3.3 and 4.2 °C. The observed changes in the calorimetric enthalpy values upon addition of nucleotide were smaller but followed in general the same trend as the changes in T_m. M765(20/+12) tends to aggregate at the low ionic strength conditions used for the DSC experiments, resulting in partial loss of the protein during sample preparation and consequently in noisier curves (Figure 2C).

Binding of Mutant Myosin Head Fragments to F-Actin. It has been suggested that DSC studies of acto-S1 offer a new and promising approach to investigate the changes that occur in the S1 molecule due to its interaction with F-actin (*22*). In the present work we applied this approach to study the

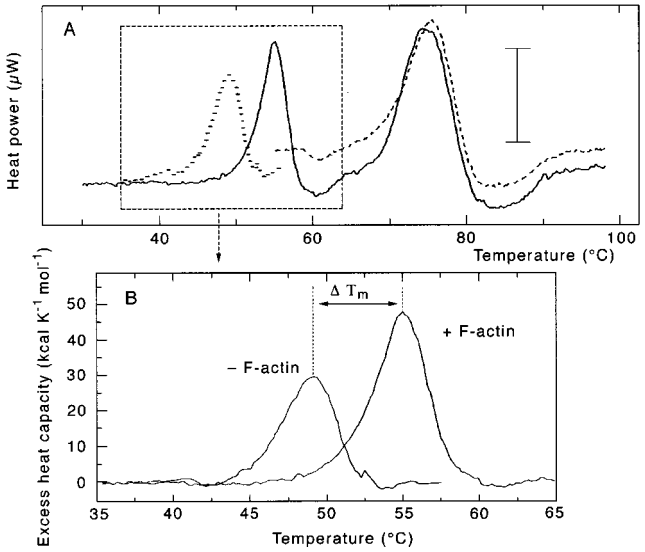

FIGURE 3: (A) The experimental DSC curves of M765 (dotted line), F-actin stabilized by phalloidin (dashed line), and their complex obtained in the presence of ADP (solid line). Conditions: 17 μM M765, 34 μM F-actin, 50 μM phalloidin in 15 mM Hepes, pH 7.3, 2 mM $MgCl_2$, 1 mM ADP, and twice-diluted G-buffer. The vertical bar corresponds to 5 μW. (B) Excess heat capacity function of M765 in the absence and in the presence of F-actin. The parameter ΔT_m (6.0 °C) is defined by the difference between denaturation temperatures of the actin-free and actin-bound myosin head fragment.

interaction of *D. discoideum* myosin head fragments with F-actin. The addition of phalloidin shifted the T_m for F-actin from 65 to 78 °C, thus providing a good separation of more than 20 °C between the calorimetric peaks of actin-bound M765 and F-actin (Figure 3A). In the absence of actin, phalloidin had no influence on the thermal denaturation of the M765.

Figure 3 shows the calorimetric trace for the thermally induced unfolding of M765 in the presence of a 2-fold molar excess of phalloidin-stabilized F-actin and ADP. While the thermal unfolding of F-actin was not significantly affected by the interaction with M765, interaction with F-actin enhanced the thermal stability of M765. This actin-induced stabilization of the myosin motor is reflected in a 6 °C shift of T_m to higher temperature and an increase in ΔH_{cal} from 220 to 285 kcal/mol (see Tables 1 and 2).

The mutant constructs showed a similar behavior. The actin-induced increase in T_m (ΔT_m) appears to correlate well with the mutant construct affinity for actin (see Table 2). The largest changes were observed for the tight binding constructs with four or more additional positive charges in loop 2. ΔT_m was determined as 8.8, 9.1, and 7.4 °C for M765(8/+4), M765(11/+6), and M765(20/+12), respectively. In contrast, actin binding to M765(20/−10) led only to a 1.2 °C increase in T_m (Figure 4). Cosedimentation and stopped-flow experiments, where M765(20/−10)-induced changes in the fluorescence of pyrene−actin were followed, confirmed that M765(20/−10) is completely bound to actin under the conditions used for the DSC experiments. A value of 130 nM was obtained for the dissociation equilibrium constant K_A, indicating that the introduction of the large negative charge in the loop 2 region led to a ∼25-fold reduction in actin affinity in comparison to the wild-type construct (see Table 2). The reduction in actin affinity was caused by an 8-fold decrease in the association rate k_{+A} to

Table 2: Calorimetric Parameters Obtained from the DSC Data for Mutant Myosin Head Fragments Complexed with F-Actin in the Presence of ADP

mutant	K_A (nM)	T_m (°C)	ΔT_m (°C)	ΔH_{cal} (kcal/mol)	$\Delta T_{0.5}$ (°C)
M765	4.8[a]	55.1	6.0	285	3.9
M765(20/−10)	125	50.3	1.2	200	4.7
M765(4/−1)	6.4[a]	55.0	3.9	290	5.5
M765(8/0)	3.7[a]	54.1	4.7	220	5.3
M765(11/0)	3.6[a]	54.4	5.1	210	4.8
M765(4/+1)	2.9[a]	55.6	6.8	235	5.7
M765(8/+4)	0.16[a]	56.8	8.8	240	3.3
M765(11/+6)	0.08[a]	54.9	9.1	250	4.2
M765(20/+12)	0.04[a]	54.4	7.4	185	5.5

[a] Values from ref *12*. Values obtained from two to four independent measurements are shown. The absolute error of the given T_m values did not exceed ±0.3 °C. The relative error of the given ΔH_{cal} values did not exceed ±10%. Experimental conditions for all measurements: 15 mM Hepes, pH 7.3, 2 mM $MgCl_2$, 1 mM ADP, and twice-diluted G-buffer.

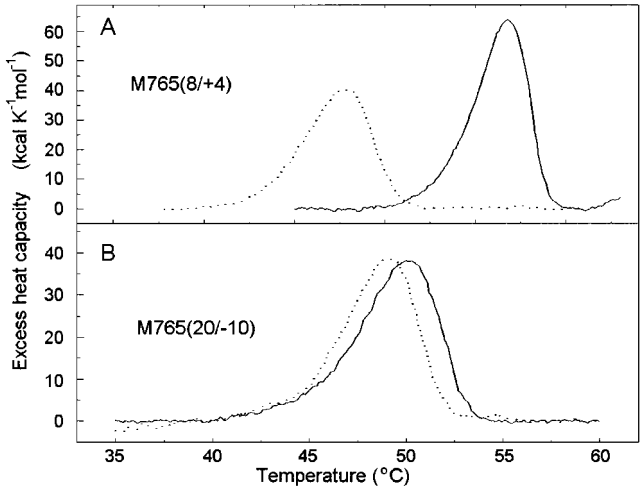

FIGURE 4: Temperature dependences of excess heat capacity for actin-bound M765(8/+4) (A) and M765(20/−10) (B) in comparison with the corresponding actin-free myosin head fragments. The temperature dependence in the presence of actin corresponds to the solid lines and that of the actin-free myosin head fragments to the dotted lines. ΔT_m = 8.8 °C for M765(8/+4), and ΔT_m = 1.2 °C for M765(20/−10). The temperature region above 60 °C, corresponding to the region of thermally induced denaturation of phalloidin-stabilized F-actin, is not shown. Conditions were the same as in Figure 3.

0.17 ± 0.1 M^{-1} s^{-1} and a 3-fold increase in the dissociation rate k_{-A} to 22.0 ± 2.0 s^{-1}. The effects of actin and ADP binding on the thermal stability of the myosin head constructs are summarized in Figure 5.

DISCUSSION

The results summarized in Table 1 suggest that lengthening of loop 2 without concomitant charge changes has only a minor effect on the thermal stability of the myosin motor domain. Insertions with up to 11 uncharged amino acid residues led only to small decreases in the transition temperature of not more than 1.8 °C. Larger reductions in transition temperature were observed with constructs M765-(20/−10), M765(11/+6), and M765(20/+12). Therefore, insertions with both multiple positive and negative charges appear to have a stronger destabilizing effect on the myosin motor domain.

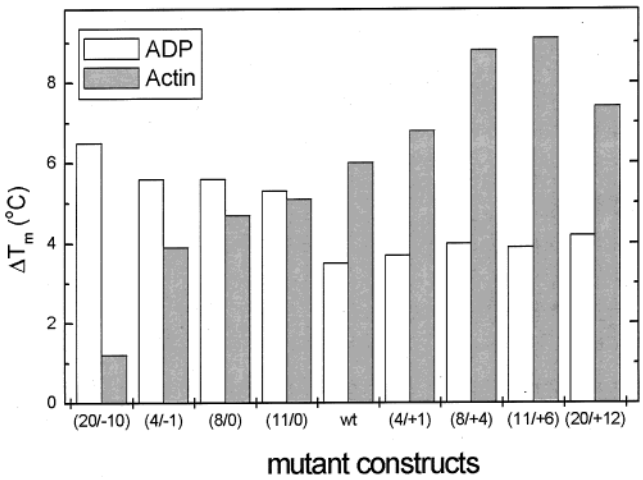

FIGURE 5: Observed shift to higher temperature (ΔT_m) of the maximum of thermal transition for myosin head fragments induced by binding to F-actin (shaded bars) and by ADP binding (open bars). Actin/ADP values (°C) are 1.2/6.5 for M765(20/−10), 3.9/5.6 for M765(4/−1), 4.7/5.6 for M765(8/0), 5.1/5.3 for M765-(11/0), 6.0/3.5 for M765, 6.8/3.7 for M765(4/+1), 8.8/4.0 for M765-(8/+4), 9.1/3.9 for M765(11/+6), and 7.4/4.2 for M765(20/+12).

Scheme 1

$$A + M(\bullet N) \underset{}{\overset{K_0}{\rightleftharpoons}} A{\sim}M(\bullet N) \overset{K_1}{\rightleftharpoons} A{-}M(\bullet N) \overset{K_2}{\rightleftharpoons} A\bullet M(\bullet N)$$

Collision complex *A state* *R state*

In the presence of excess ADP, a good correlation between the construct charge, actin affinity, and thermal stability was observed for the thermal unfolding of the myosin motor domain constructs strongly bound to actin (Table 2). The fact that construct M765(20/+12), possessing the highest affinity for actin, displayed a smaller actin-induced increase in the thermal transition temperature than M765(8/+4) and M765(11/+6) indicates that the relative contributions of a stabilizing increase in actin affinity and the destabilizing effect of inserting multiple residues and charges are complex and difficult to predict. However, the correlation between actin affinity and thermal stability displayed by the other constructs is sufficiently strong to suggest that loop 2-mediated charge−charge interactions with actin play an important role in the stabilization of the R-state complex. This conclusion is in good agreement with transient kinetics data that showed that insertion of four or more basic amino acids leads to a large increase in the affinity of the myosin motor domain for F-actin, resulting from changes in both k_{+A} and k_{-A} (*12*). The association and dissociation rate constants for binding of the myosin motor domain to F-actin, k_{+A} and k_{-A}, as determined by transient kinetics, reflect the three-step process of formation and stabilization of the actomyosin complex originally formulated for skeletal muscle myosin (*31*) (Scheme 1).

In this model the apparent rate constants k_{+A} and k_{-A} correspond to complex terms that are comprised of more than one intrinsic rate constant, with k_{+A} corresponding to K_0k_{+1} and k_{-A} to $k_{-1}/(1 + K_2)$. Therefore, the observed changes in k_{+A} and k_{-A} suggest that faster formation of a collision complex and stabilization of the R-state are equally responsible for the increase in actin affinity of mutant constructs with a positively charged loop 2 region.

Binding of ADP has been shown to increase the thermal stability of the myosin motor by shifting the thermal transition to higher temperature (*21*). All mutant constructs showed the expected shift of the thermal transition to higher temperature upon addition of ADP (Figure 2, Table 1). The extent of the ADP-induced stabilization varied between 3.5 °C for the wild-type construct M765 and 6.5 °C for M765-(20/−10). In the presence of ADP, several mutant constructs displayed similar or higher transition temperatures than the wild-type construct M765 (49.1 °C), and the highest transition temperature of 51.1 °C was measured for M764(4/−1). Constructs with loop 2 carrying additional positive charges showed a similar degree of thermal stabilization as the wild-type construct M765, whereas constructs with neutral or acidic residue loop extensions showed a 50−85% greater increase in ΔT_m. The constructs showing the largest increase in the ADP-induced ΔT_m are those with the smallest increase in actin-induced ΔT_m (Figure 5). In general, the construct behavior upon binding of ADP lends support to the idea that loop 2 affects communication between the actin- and nucleotide-binding sites.

Formation of the ternary complexes of mutant myosin head fragments with ADP and V_i or BeF_3 produced a further increase in the thermal stability of all constructs (Table 1). Since the complexes with V_i or BeF_3 are believed to be stable analogues of the myosin ATPase intermediates M·ADP·P_i and M·ATP (*27*−*30*), the changes in thermal unfolding induced by formation of these complexes reflect structural changes that occur during the course of the ATPase reaction (*20*, *21*). Despite some variability in the effects of V_i and BeF_3 on the thermal unfolding of the mutant myosin head fragments (Table 1), all constructs were clearly able to undergo structural changes due to the formation of stable ternary complexes with ADP and P_i analogues. In general, this is consistent with the enzymatic properties of these constructs as described in an earlier study (*12*). All mutant constructs are able to hydrolyze ATP at least as fast as M765, and changes in the loop 2 region do not directly affect nucleotide binding (*12*, *32*, *33*). However, they affect coupling between the nucleotide-binding site and the actin-binding site, as reflected by a 35−70-fold increase in the apparent second-order rate constant k_{cat}/K_{app}, which was observed in steady-state experiments for the actomyosin ATPase of constructs M765(8/+4), M765(11/+6), and M765(20/+12) (*12*). Therefore, the changes in the thermal unfolding induced by nucleotide or actin binding stem at least in part from conformational changes in the communication zone between the nucleotide- and actin-binding sites of the myosin motor domain.

In conclusion, the DSC data presented here lend strong support to a role of the loop 2 region in the stabilization of the R-state and in determining the structural changes that are associated with the coupling of information between the actin- and nucleotide-binding sites.

ACKNOWLEDGMENT

We thank S. Zimmermann for expert technical assistance and the generation of expression vectors for the mutant constructs and J. Wray for critical reading of the manuscript and discussions. D.J.M. and M.F. thank K. C. Holmes for continual support and encouragement.

REFERENCES

1. Toyoshima, Y. Y., Kron, S. J., MaNally, E. M., Niebling, K. R., Toyoshima, C., and Spudich, J. A. (1987) *Nature 328*, 536−538.
2. Manstein, D. J., Ruppel, K. M., and Spudich, J. A. (1989) *Science 246*, 656−658.
3. Sellers, J. R., and Goodson, H. V. (1995) *Protein Profile 2*, 1323−1423.
4. Spudich, J. A. (1994) *Nature 372*, 515−518.
5. Schröder, R. R., Manstein, D. J., Jahn, W., Holden, H., Rayment, I., Holmes, K. C., and Spudich, J. A. (1993) *Nature 364*, 171−174.
6. Chaussepied, P., and Morales, M. F. (1988) *Proc. Natl. Acad. Sci. U.S.A. 85*, 7471−7475.
7. Yamamoto, K. (1989) *Biochemistry 28*, 5573−5577.
8. Yamamoto, K. (1990) *Biochemistry 29*, 844−848.
9. DasGupta, G., and Reisler, E. (1989) *J. Mol. Biol. 207*, 8333−836.
10. Cheung, P., and Reisler, E. (1992) *Biochem. Biophys. Res. Commun. 189*, 1143−1149.
11. Uyeda, T. Q. P., Ruppel, K. M., and Spudich, J. (1994) *Nature 368*, 567−569.
12. Furch, M., Geeves, M. A., and Manstein, D. J. (1998) *Biochemistry 37*, 6317−6326.
13. Privalov, P. L., and Potekhin, S. A. (1986) *Methods Enzymol. 131*, 4−51.
14. Shnyrov, V. L., Sanchez-Ruiz, J. M., Boiko, B. N., Zhadan, G. G., and Permyakov, E. A. (1997) *Thermochim. Acta 302*, 165−180.
15. Goodno, C. C. (1982) *Methods Enzymol. 85*, 116−123.
16. Phan, B., and Reisler, E. (1992) *Biochemistry 31*, 4787−4793.
17. Werber, M. M., Peyser, Y. M., and Muhlrad, A. (1992) *Biochemistry 31*, 7190−7197.
18. Levitsky, D. I., Shnyrov, V. L., Khvorov, N. V., Bukatina, A. E., Vedenkina, N. S., Permyakov, E. A., Nikolaeva, O. P., and Poglazov, B. F. (1992) *Eur. J. Biochem. 209*, 829−835.
19. Bobkov, A. A., Khvorov, N. V., Golitsina, N. L., and Levitsky, D. I. (1993) *FEBS Lett. 332*, 64−66.
20. Bobkov, A. A., and Levitsky, D. I. (1995) *Biochemistry 34*, 9708−9713.
21. Levitsky, D. I., Ponomarev, M. A., Geeves, M. A., Shnyrov, V. L., and Manstein, D. J. (1998) *Eur. J. Biochem. 251*, 275−280.
22. Nikolaeva, O. P., Orlov, V. N., Dedova, I. V., Drachev, V. A., and Levitsky, D. I. (1996) *Biochem. Mol. Biol. Int. 40*, 653−661.
23. Manstein, D. J., Schuster, H.-P., Morandini, P., and Hunt, D. M. (1995) *Gene 162*, 129−134.
24. Manstein, D. J., and Hunt, D. M. (1995) *J. Muscle Res. Cell Motil. 16*, 325−332.
25. Spudich, J. A., and Watt, S. (1971) *J. Biol. Chem. 246*, 4866−4871.
26. Le Bihan, T., and Gicquaud, C. (1991) *Biochem. Biophys. Res. Commun. 181*, 542−547.
27. Fisher, A. J., Smith, C. A., Thoden, J., Smith, R., Sutoh, K., Holden, H. M., and Rayment, I. (1995) *Biophys. J. 68*, 19s-28s.
28. Ponomarev, M. A., Timofeev, V. P., and Levitsky, D. I. (1995) *FEBS Lett. 371*, 261−263.
29. Smith, C. A. and Rayment, I. (1996) *Biochemistry 35*, 5404−5417.
30. Phan, B. C., Peyser, Y. M., Reisler, E., and Muhlrad, A. (1997) *Eur. J. Biochem. 243*, 636−642.
31. Geeves, M. A. and Conibear, P. B. (1995) *Biophys. J. 68*, 194s-201s.
32. Murphy, C. T. and Spudich, J. A. (1999) *Biochemistry 38*, 3785−3792.
33. Knetsch, M. L. W., Uyeda, T. Q. P., and Manstein, D. J. (1999) *J. Biol. Chem. 274*, 20133−20138.

BI992420A